III International Conference on Particle-based Methods – Fundamentals and Applications
PARTICLES 2013
M. Bischoff, E. Oñate, D.R.J. Owen, E. Ramm & P. Wriggers (Eds)

# MATERAL POINT METHOD FOR GEOTECHNICAL PROBLEMS INVOLVING LARGE DEFORMATION

**RAYDEL LORENZO[*], RENATO P. CUNHA[2] AND MANOEL P. CORDÃO NETO[3]**

[*] PhD. Student. University of Brasilia
Campus Darcy Ribeiro, SG12 Brasilia, Brasil
raydellr@gmail.com, www.geotecnia.unb.br/gpfees

[2] Professor. University of Brasilia
rpcunha@unb.br , www.geotecnia.unb.br/gpfees

[3] Professor. University of Brasilia
mporfirio@gmail.com, www.geotecnia.unb.br

**Key words:** Geotechnical Problems, MPM, GIMP, Large Deformation.

**Abstract.** In geotechnical engineering and foundations there are problems that involve large deformations, contact between bodies and penetration. In this case, Material Point Method (MPM) can be an alternative to Finite Element Method (FEM), improving considerably the quality of analysis. The MPM models the soil as a group of Lagrangean particles that are moved over a fix Eulerian mesh. Thus, the aspect related to distortions that arise in large deformation problems are solved. There are several codes of MPM. In this paper a code called NairnMPM is used. It allows the performance 2D and 3D dynamic analyses and can handle any defined material type. A very well-known geotechnical model (Modified Cam Clay) was implemented within the NairnMPM, being demonstrated through the results of oedometric and tri-axial tests. Also, a plane strain simulation of a rigid footing resting over a horizontal Modified Cam Clay soil is depicted after its submission to large settlement levels, in order to verify the method's ability to handle large deformations problems.

## 1 INTRODUCTION

In geotechnics there are problems of difficult simulation that involve large deformation. Typical of these are debris flows, landslides, pile foundation tests, most types of in situ tests (CPT, DMT, SPTs), or dynamic pile driving. They are generally analysed by simplified methods, as cavity expansion theories or simply ignored at all (interpreted empirically or by plain analytical rules) [1].

In the last years the finite element method (FEM) have become the standard tool for solve the majority of the analyses in solid mechanics. Nevertheless, this method, in its traditional Lagrangian formulation, is definitively not suitable to deal with large deformed meshes.

According to [2] when aforementioned problems are simulated with this formulation, great distortions of the mesh occur and some sort of remesh can be required. During remesh process all the state variables need to be mapped from the distorted mesh to the new defined one. This can lead to the introduction of numerical errors in the calculation [3].

To solve the difficulties with FEM usage on large deformation problems, particular mesh less methods have been developed. Within these advanced methods, the generation of the mathematical problems reduces to the generation of material points and his distribution, without fix connectivity between them. Within this category of mesh-less methods are the discrete element method (DEM), the smooth particle hydrodynamics (SPH) and the particle in cell method (PIC) [4]. Each of these methods has advantages and disadvantages in the simulation of solid mechanics in large deformation levels. Some are then associated with the properties or characterization of solid materials as in DEM, others with the delineation of material boundaries, as in PIC.

The Material Point Method is a type of PIC [5]. It combines ideas and procedures of both particle and finite element methods. It has the potential advantages of using the Lagrangian and Eulerian descriptions of kinematic. With the MPM a body is modelled as a group of Lagrangian particles. These particles transport the state variables and other variables needed to solve the kinematic equations. The variables are interpolated from particles related to a fixed mesh in which the equations of motion will be solved. After the solution is obtained, it's interpolated to the particles and the state variables and positions are updated. This procedure is repeated throughout the time domain of the problem, hence leading to a fixed mesh with no distortion at all [1].

In the last decade a generalization of the MPM was done to eliminate the numerical noise that arises when a particle crosses from one cell to another. This method is known as the Generalized Interpolation Material Point (GIMP), and was introduced by [6]. New interpolation functions were introduced with a domain larger than a cell, allowing particle movement tracking when it goes out of its original cell.

In the present paper a code of GIMP developed by [7] called NairnMPM is used and verified. This code allows 2D and 3D dynamic analyses with any defined material. A very well-known critical state model (Modified Cam Clay) is implemented within the GIMP in a way that allows introducing more advanced geotechnical models in a simple manner. Details of the model implementation, and certification results derived from the comparison with tri-axial and oedometric path are presented and discussed. The paper finalizes with a plane strain simulation of a rigid footing resting over a horizontal Modified Cam Clay soil and the results are compared with those presented by [8].

## 2 OVERALL PROCEDURE OF MPM

Although a very good discussion on the *implicit* time integration for MPM is presented in [9], the majority of the codes found in the literature are *explicit*. In the present paper the explicit solution in time is commented and adopted.

The numerical process for solving kinematic problems in the MPM can be compacted to four steps; 1-initialization of particles, 2- Integration of constitutive equations, 3- Solution of momentum conservation and 4- Update of material points. Detailed algorithms of the MPM can be found in [10]. In general, all algorithms follow these four basic steps, except for the position in time when the integration of the constitutive equation is done. In [11] two approaches for the stress-update respectively denominated USL (Update Stress Last) and USF (Update Stress First), are presented (see Figure 1). The difference in the solutions using these methods is related to the energy point of view. In [12] attention is focused in the numerical characteristics of these methods. It is found that the USF approach gives a better conservation of the energy than the USL approach. In the NairnMPM code another technique is presented and recommended [10]. It is named USAVG (Update Stress Average), and it does an update of the stresses before solve the momentum equation and in the final of the time step. Notice that in this method the stresses and strains are updated two times, however with the half of the time step value at each time. For the analyses carried out in the present paper no differences were obtained for any of the three aforementioned approaches, although the USAVG techniques needed more calculation time. Although in [10] is shown that these methods generate different results in terms of energy values of the particles, this is important in fracture analyses, but it is not so relevant in the type of analyses related to the present paper.

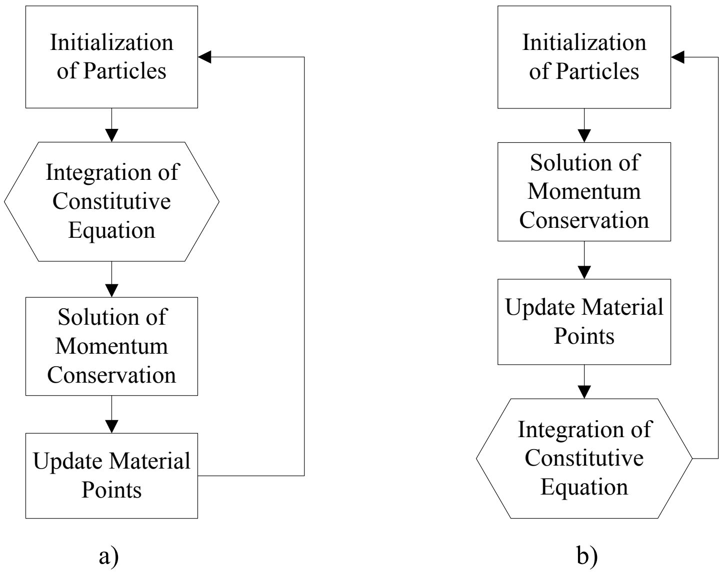


**Figure. 1.** General algorithm of MPM. a) Update Stress First Algorithm b) Update Stress Last.

The formulation of the method applied to kinematic problems can be found in elsewhere [10], where particular details of the implementations are presented in [12].

## 3 CRITICAL STATE MODELS

Critical States theory, as presented by [13], postulate that the material flows as a frictional fluid at constant specific volume when, the effective isotropic pressure, and axial-deviator stress, have an specific relation that is a property of the material, and the specific volume have a value related to the effective isotropic pressure and some initial conditions. This concept was initially introduced by Roscoe in the 1960s and is the base of several existing different models. They combine five concepts in only one theory, wich are:

1- Relation between void ratio and effective isotropic stress.
2- Plastic volumetric strain in different trajectories of stresses, including isotropic and shearing.
3- Critical State.
4- Failure criteria.
5- Hardening and softening.

One of the first and most used critical state models is the Modified Cam Clay (MCC). This model was developed by [14] and represents a slight extension of Cam Clay model by adopting a revised work equation to derive the yield function and plastic potential [13].

The yield surface of the model is defined in the p-q plane as forming an ellipse.

$$f = M^2\left(p^2 - p_0 p'\right) + q^2 \tag{1}$$

Where $M$ is the slope of the critical state line, $p_0$ is the pre-consolidation stress, $p$ is the isotropic stress and $q$ the deviator stress. Hardening is defined as a function of the plastic volume deformation ($\varepsilon_v^p$) in the following form:

$$\frac{dp_0}{p_0} = \frac{(\lambda - \kappa)}{(1+e)}\varepsilon_v^p \tag{2}$$

Where $\lambda$ is the slope of the normal compression line in the space of the logarithmic mean stress $\ln p'$ versus the void ratio $e$. $\kappa$ the slope of the unloading-reloading line in the $\ln p' - e$ space.

It is assumed an associated flow rule, i.e. $f(\sigma, p_0) = g(\sigma, p_0)$, where $g(\sigma, p_0)$ is the plastic flow function and $\sigma$ the Cauchy stress tensor.

The elastic part of the model is non-linear, with the elastic rigidity matrix changing with $p$. If a tangent elastic modulus is assumed, it can be expressed by the following manner:

$$E = \frac{3(1-2\nu)(1+e)}{\kappa}p \tag{3}$$

The second elastic constant can be chosen by assuming either a constant Poisson's ratio($\nu$) or an assumed constant value of shear modulus ($G$).

This model is capable of considering the most important features of the soil behaviour. In the last twenty years a lot of improvement has taken place in order to allow the consideration of other characteristics of the natural soils. Some of them are presented from [16–18] and for instance include an extension to the general stress space, a modified failure criteria, and a non-associated flow rule to simulate structured soils.

## 4 STRESS INTEGRATION OF THE MODEL

As in FEM analyses, in MPM a set of ordinary differential equations must be solved to find the stress variation based on the strain increment. In the MPM case, the strain increment comes from the velocities calculated at the nodes of the fixed mesh. The system of equations is normally written in a rate form, as follow:

$$\begin{aligned} \dot{\underset{\approx}{\sigma}} &= \underset{\approx\approx}{D} : \dot{\underset{\approx}{\varepsilon}} \\ \dot{h} &= H\left(\underset{\approx}{\sigma}, h\right)\dot{s} \end{aligned} \tag{4}$$

Where $\sigma$ is the Cauchy stress tensor, $D$ the elasto-plastic stress-strain matrix, $\varepsilon$ the strain tensor, $h$ an internal stress variable of hardening and $s$ an internal strain variable of hardening. In the Modified Cam Clay $h$ is $p_0$ and $s$ is $\varepsilon_v^p$.

Equation (4) has to be integrated for each time step in a strain domain. Actually this system of equations is solved on an incremental form, because the mathematical complexities from most models do not allow a direct integration. In an incremental form this equation is expressed as:

$$\underset{\approx}{\sigma}^{t+\Delta t} = \underset{\approx}{\sigma}^{t} + \underset{\approx\approx}{D} : \Delta\underset{\approx}{\varepsilon} \tag{5}$$

Several integration schemes have been proposed to solve this system of equations. In [19] it is presented an explicit algorithm with substepping and error control with good results in terms of efficiency and accuracy. In the present paper the simple explicit forward Euler algorithm was implemented as a first step to test the model. Nevertheless, further implementations will need a more efficient algorithm.

In the case of large deformation analyses, the integration of the constitutive equations can no longer be done by equation (5). Some modifications have to be done to avoid changes in the stress tensor due to rigid-body motion [20]. One of the most used modifications is the introduction of an objective stress rate. If the hypoelasticity is used, the Jaumann stress rate is introduced in the stress-strain relations, wish is defined as follows:

$$d\underset{\approx}{\sigma}^{J} = d\underset{\approx}{\sigma} - d\underset{\approx}{\Omega}\cdot\underset{\approx}{\sigma} - \underset{\approx}{\sigma}\cdot d\underset{\approx}{\Omega}^{T} = \underset{\approx\approx}{D} : d\underset{\approx}{\varepsilon} \tag{6}$$

where $\underset{\approx}{\Omega}$ is the non-symmetric part of the displacement gradient.

The stress increment is found by integrating $d\underset{\approx}{\sigma}$ in equation(6). In an incremental form this can be written as:

$$\hat{\underset{\approx}{\sigma}}^{t+\Delta t} = \underset{\approx}{\sigma}^{t} + \Delta\underset{\approx}{\Omega}\cdot\underset{\approx}{\sigma}^{t} + \underset{\approx}{\sigma}^{t}\cdot\Delta\underset{\approx}{\Omega}^{T} + \underset{\approx\approx}{D}\left(\underset{\approx}{\sigma}^{t}, {}^{t}\varepsilon_{v}^{p}\right) : \Delta\underset{\approx}{\varepsilon} \tag{7}$$

In equation (7), the first three terms of the right side represent the previous stress state in the present configuration, where the second and third terms take into account the possible rigid body rotations. Equation (7) is a simplification of:

$$\hat{\underset{\approx}{\sigma}}^{t+\Delta t} = R\underset{\approx}{\sigma}^{t}R^{T} + \underset{\approx\approx}{D}\left(\underset{\approx}{\sigma}^{t}, \varepsilon_{v}^{p}\right) : \Delta\underset{\approx}{\varepsilon} \tag{8}$$

In which $R$, is the rotation matrix. A simplification is introduced ignoring the $\Delta t^2$ terms when deducing equation (7) from equation (8).

One can notice that, introducing in this manner the effect of the rigid motion in the integration scheme, the algorithm to be used for small deformation analysis need only to be modified with a subroutine that calculates the part of rigid body rotation, keeping all previous implementations.

In [21] three different ways to introduce the rigid motion effects are presented, i.e. before, after or during the integration of the constitutive equations. No differences in the accuracy of results obtained by these algorithms was observed in [21]. For the analyses done in the present paper, the correction of the stress tensor is done after the constitutive equations are integrated.

### 4.1 Method of projecting back

The integration of the constitutive equations of an elasto-plastic model is normally done in an incremental form, as mentioned before. All the process of integration is done assuming a constant constitutive matrix. Because the constitutive matrix changes with the level of stress and the hardening parameter, it is required to assume small steps of integration in the numerical procedure. In general the procedure is to assume an elastic predictor and a plastic correction of the stress state. Even with the use of small steps, in the post yield range, it is found in practice that the predicted state of stress at the end of a loading increment may not lead to the correct yield surface. This deviation is found to be more pronounced in critical state models because the yield surface is also moving during the loading increment [22]. Given such feature it is necessary to introduce a method for projecting back the state of stress to the yield surface. Five different methods are then proposed in [22]. In the present paper one of these methods will be employed, which allows the stress state to be projected back along the plastic flow direction. Therefore, the algorithm of integration is mathematically expressed as:

$$d\underset{\approx}{\sigma}^{trial} = \underset{\approx}{\underset{\approx}{D}}^{E} : d\underset{\approx}{\varepsilon} \tag{9}$$

$$\underset{\approx}{\sigma}^{trial} = \underset{\approx}{\sigma}^{t} + d\underset{\approx}{\sigma}^{trial} \tag{10}$$

If $f\left(\sigma^{trial}, p^{t}{}_{0}\right) > 0$ a plastic correction is then needed,

$$\underset{\approx}{\sigma}^{t+\Delta t} = \underset{\approx}{\sigma}^{t} + d\underset{\approx}{\sigma}^{trial} - \underset{\approx}{\underset{\approx}{D}}^{E} : d\underset{\approx}{\varepsilon}_{p} = \underset{\approx}{\sigma}^{t} + d\underset{\approx}{\sigma}^{trial} - \underset{\approx}{\underset{\approx}{D}}^{E} : \lambda_{p}\frac{\partial g}{\partial \underset{\approx}{\sigma}^{trial}} \tag{11}$$

Verified if

$$-ftol < f\left(\sigma^{t+\Delta t}, p_{0}{}^{t+\Delta t}\right) < ftol \tag{12}$$

If not, the return correction algorithm shall be applied, as follow:

$$\underset{\approx}{\bar{\sigma}}^{t+\Delta t} = \underset{\approx}{\sigma}^{t+\Delta t} - \alpha_{c}\left(\frac{\partial g}{\partial \sigma^{t+\Delta t}}\right) \tag{13}$$

$\alpha_c$ is and scalar quantity and can be computed as:

$$\alpha_{c} = \frac{f\left(\sigma^{t+\Delta t}, p_{0}{}^{t+\Delta t}\right)}{\left(\frac{\partial f}{\partial \sigma^{t}}\right)^{T}\left(\frac{\partial g}{\partial \sigma^{t}}\right)} \tag{14}$$

At this stage, it is verified the value of the yield function at the corrected stress state( $\bar{\sigma}^{t+\Delta t}$ ) and if it is within the desired tolerance ( $ftol$ ). If not, then the return correction algorithm shall be applied again, in order to change the values of the stresses according to:

$$\begin{aligned} \underset{\approx}{\sigma}^{t+\Delta t} &= \underset{\approx}{\bar{\sigma}}^{t+\Delta t} \\ \underset{\approx}{\sigma}^{t} &= \underset{\approx}{\sigma}^{t+\Delta t} \end{aligned} \tag{15}$$

Finally, yielding the corrected value $\underset{\approx}{\bar{\sigma}}^{t+\Delta t}$ .

This stress state needs to be modified to take into account the possible rigid body motion. Once it is projected back, the correction presented in equation(7) can be applied.

In summary, this item explained an algorithm for the integration of critical state models. Four stages; First, a "trial" elastic-based state; second, a correction for plastic strains; third, correction to return the state stress to the yield surface; and a final fourth stage, where another correction is done in regard to a possible rigid-body motion. In next section this particular algorithm will be tried out in some basic analyses.

## 5 VALIDATION OF THE IMPLEMENTED MODEL

As stated before, the Modified Cam Clay model was implemented in a code of GIMP, called NairnMPM code. This code was developed by Professor John Nairn at the University of Oregon. The code is explicit and allows 2D and 3D numerical analyses. It was written in C++ and incorporates distinct material models, especially those related to mechanical and wood engineering. More details about the NairnMPM can be found in [7].

In this paper, a new class of material, called GeoMaterial, was created. It allows the addition of critical state models in a simple way. The integration of the constitutive equations follows the steps already described before. The Modified Cam Clay model was implemented as a simple model to verify the implementation of this new class of (earth-like) material. Simulations with known stress path were conducted to test the model and validate it.

Figure 2 presents an oedometric path obtained with the GIMP code using the MCC model. The present analysis began from the null stress state. The critical state line (CSL) and the projection of the yield surface in this plane are also depicted. In this figure it is also shown the simulated stress path achieved by the numerical model and the one obtained by the integration of the MCC. This last one is considered the “exact” for comparison. It is clearly seen that the results obtained are good for an engineering purpose. The curvature of the path, when it touches the yield surface (figure 2. a), is an outcome of the associated flow rule of the implemented model. The direction of the stresses is the same of the strains direction, a time step before the stress state touches the yield surface Nevertheless, when the elasto-plastic behaviour begins, the direction of the plastic part of the strains is perpendicular to the plastic flow surface (equal to yield surface) and it does not have the same direction of the stresses, giving this deviation from the original trajectories of stresses. This curvature is corrected when the plastic strains are much larger than the elastic ones.

Figure 3 presents a tri-axial stress path simulation of a sample with an over consolidated ratio (OCR) in the dry side of the yield function. This path is done to check the implementation of the method in terms of projecting back. The trajectories in the $p$ *vs* $q$ plane and the $q$ *vs* $\varepsilon_d$ are presented. Notice that $\varepsilon_d$ is the deviatory strain. The trajectories are presented for the calculation which adopts, and without adopting, the method of projecting back (i.e. with and without return algorithm).

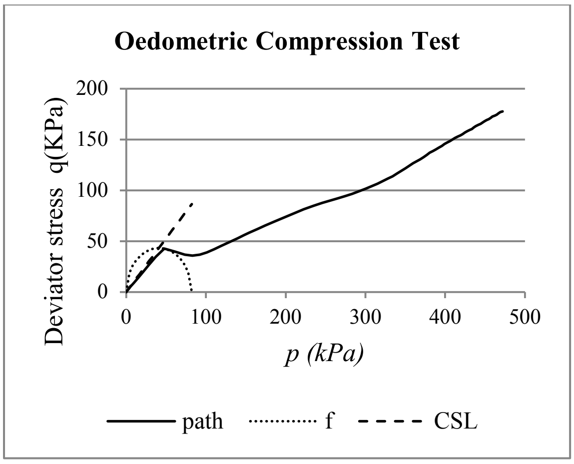


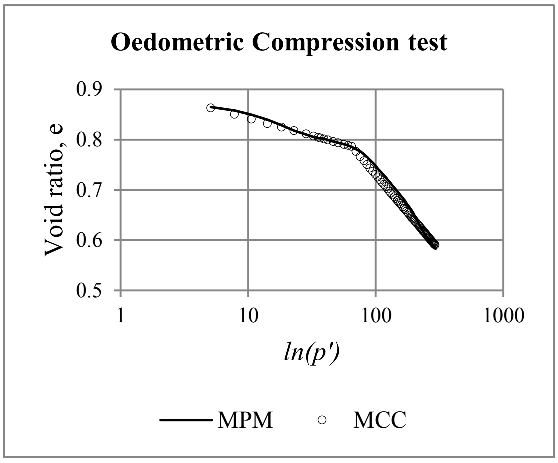


a) b)

**Figure 2**: Oedometric compression path. a)*p-q space* b) *lnp-e space.*

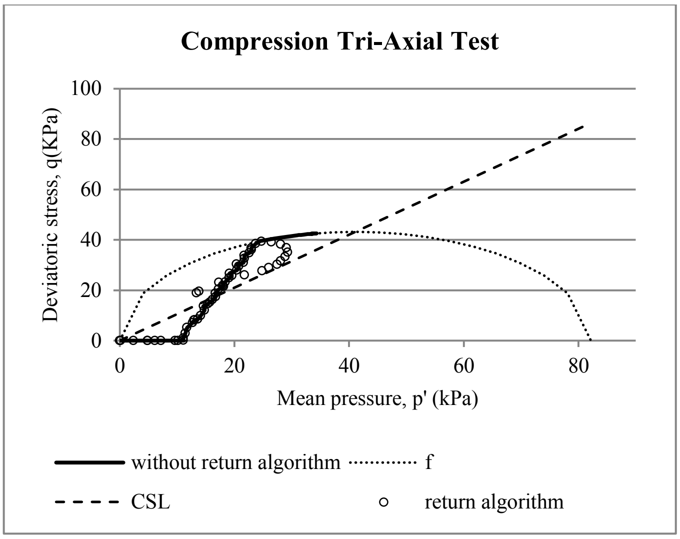


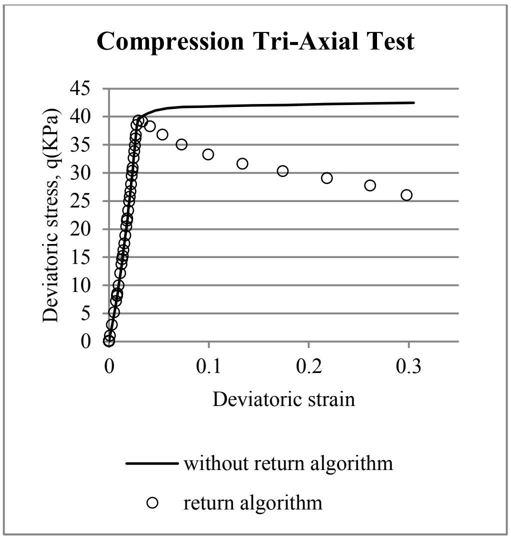


a) b)

**Figure 3**: Compression tri-axial test in the supercritical side. a) *p-q space* b) $q\ vs\ \varepsilon_d$ .

The results are as expected. The trajectory obtained by using the return algorithm presents a softening feature once it reaches the critical state line. With the time step which has been used in these examples, it was necessary only two or three iteration to have the stress state correctly returned to the yield surface.

The problems associated with the MCC model have not been commented herein because the emphasis of the present paper was solely on the implementation of the model. Nevertheless, it wouldn't be difficult to introduce some of the new improvements associated with the MCC model, which will be, surely, left for a future stage.

## 6 NUMERICAL EXAMPLE

The potential use of the algorithm is also tested against a hypothetical load test case. The example consists of a rigid footing resting in MCC soil submitted to large settlement levels. This case is particularly characterized by strong rotations, hence, being well suitable to test the applicability of the numerical method and the implemented model.

The properties and the geometry of the problem are presented in Figure 4, where $k_0$ is the earth pressure coefficient at rest, $\gamma$ is the unit weigh of the soil, $\phi$ is the internal friction angle which relates with $M$ , and $\delta$ is the applied prescribed settlement. The assumed size of the footing B is equal to 1m.

As mentioned in [8], as the soil has no strength at zero stress, in according to the MCC model, its self-weight is used to generate a non-zero initial stress field. In addition, a thin layer (0.25m in thickness) of elastic material is added on top of the MCC soil, in order to avoid a slope failure problem when the settlement of the footing is large enough. That means a slope failure of the adjacent soil once it becomes highly inclined.

For this example, 4 particles by cell are adopted, for a total of 10010 particles and a structured square uniform mesh with cell length of 200mm. The GIMP (uGIMP) method is used as described in [6] and the integration of the constitutive equation is employed as previously addressed in section 4.

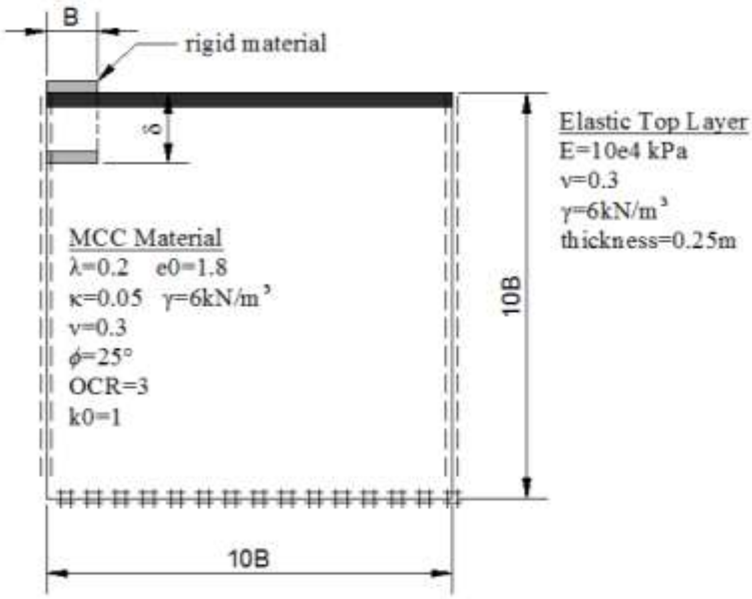


**Figure 4:** Rigid Footing in MCC soil (modified of [8]).

This example is also documented in [8] and the results obtained by his authors are used herein as comparison. They used ALE and Update Lagrange methods for solving this problem that involve large deformations. Also two objectivity stress rate tensor in the integration of the constitutive equation were used. These are respectively Jaumann stress rate and another one that is equivalent to Truesdell stress rate (see [8] for more detail). The predicted average vertical pressure under the footing *vs* displacement curve is showed in Figure 5. In Figure 6 the both final deformation level and vertical displacement shade are presented.

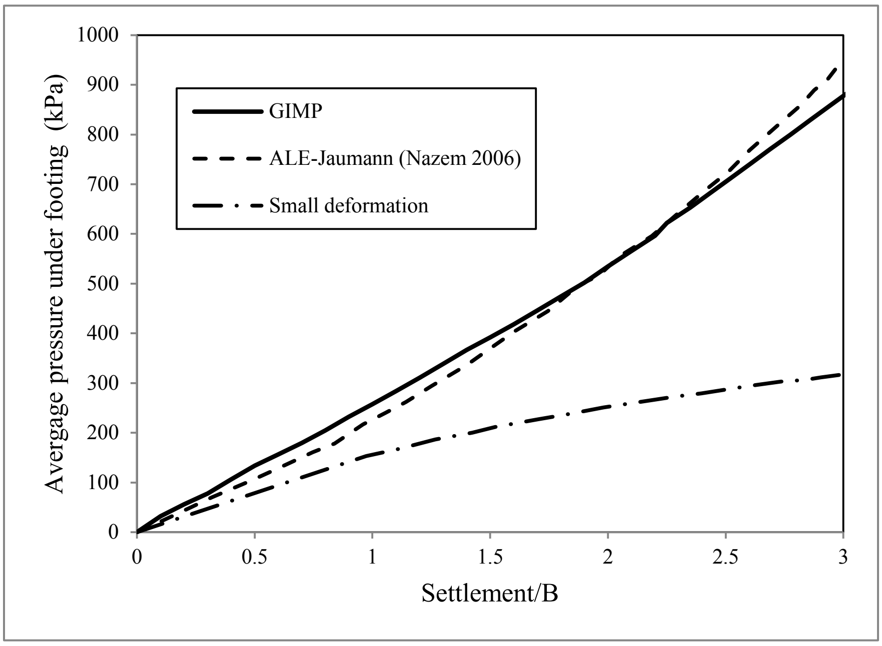


**Figure 5:** Load displacement response of a rigid rough footing on the MCC soil.

The prescribed displacement was applied very slowly for avoid oscillations problems in the model, because of this no damping was required to preclude this problem. The analysis needed a total CPU time of 3 hours. The constant time step was computed using the Courant condition with a deformation moduli of 10MPa.

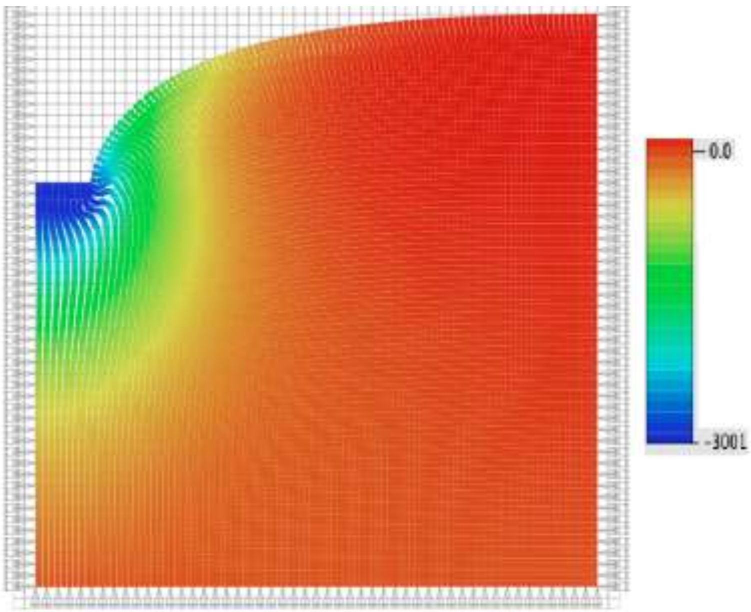


**Figure 6:** Deformed shape and vertical displacement (mm) for footing in MCC soil.

As shown, the GIMP method seems to be stable for large deformations and rotations, at least for the range of magnitudes attained in this particular example.

The results obtained herein with GIMP are very similar to the ones predicted by [8]. Nevertheless, some minor differences can be attributed to the inherent proper characteristics of the adopted numerical methods.

## 7 CONCLUSIONS

A new class of materials that allows including more suitable models for the simulation of geotechnical problems was introduced in the context of GIMP. Some key conclusions are drawn from the numerical examples considered in this paper:

- The new GeoMaterial class provides a frame for the introduction of critical states models in the NairnMPM code based in the GIMP.
- The numerical example problem developed involved large displacement and rotations of the elasto-plastic medium. The GIMP and the Jaumann stress rate seem to provide an effective solution to this type of problems.
- The next step is to implement a non-constant time step algorithm based in the magnitude of deformations. Also, a substepping algorithm to integrate the constitutive model is required.

## ACKNOWLEDGEMENTS

The authors acknowledge the support of the National Brazilian Agency CNPq and the Geotechnical Graduation Prog. of the UnB for all related funds that allowed this particular research.

## REFERENCES

[1] W. Kuen, “Numerical simulation of landslides and debris flows using an enhanced material point method,” University of Washington, 2009.

[2] L. Beuth, T. Benz, and P. A. Vermeer, “Large deformation analysis using a quasi-static Material Point Method,” pp. 1–6, 2007.

[3] C. J. Coetzee, “The Modelling of Granular Flow Using the Particle-in-Cell Method,” University of Stellenbosch, 2004.

[4] F. Zabala, “Modelación de problemas geotécnicos hidromecánicos utilizando el método del punto material,” Universidad Politécnica de Catalunya, 2010.

[5] D. Sulsky, Z. Chen, and H. L. Schreyerb, “A Particle Method for History-Dependent Materials,” *Computer Methods in Applied Mechanics and Engineering*, vol. 118, no. 1, pp. 179–196, 1994.

[6] S. G. Bardenhagen and E. M. Kober, “The Generalized Interpolation Material Point Method,” *Tech Science Press*, vol. 5, no. 6, pp. 477–495, 2004.

[7] J. Nairn, “Source code and documentation for NairnMPM Code for Material Point Calculations. http://oregonstate. edu/~nairnj/.” 2011.

[8] M. Nazem, D. Sheng, and J. P. Carter, “Stress integration and mesh refinement for large deformation in geomechanics,” *International Journal for Numerical Methods in Engineering*, vol. 65, no. 7, pp. 1002–1027, Feb. 2006.

[9] D. Sulsky and A. Kaul, “Implicit dynamics in the material-point method,” *Computer Methods in Applied Mechanics and Engineering*, vol. 193, no. 12–14, pp. 1137–1170, Mar. 2004.

[10] J. Nairn, “Material Point Method Calculations with Explicit Cracks,” *Computer Modeling in Engineering and Sciences*, vol. 4, no. 6, pp. 649–663, 2003.

[11] S. G. Bardenhagen, “Energy Conservation Error in the Material Point Method for Solid Mechanics,” *Journal of Computational Physics*, vol. 180, no. 1, pp. 383–403, Jul. 2002.

[12] O. Buzzi, D. M. Pedroso, and A. Giacomini, “Caveats on the Implementation of the Generalized Material Point Method,” *Tech Science Press*, vol. 31, no. 2, pp. 85–106, 2008.

[13] A. Schofield and P. Wroth, *Critical State Soil Mechanics*. Cambridge: Wiley, p. 229.

[14] Roscoe and Burland, “On the generalised stress-strain behaviour of ‘wet clay’,” *Engineering Plasticity*, pp. 535–609, 1968.

[15] A. Gens and D. M. Potts, “Modelos Elasto-Plasticos de Estado Critico para Análisis Numerico de Problemas Geotecnicos. I-Formulasción Básica y Principales Modificaciones,” *Revista internacional de Métodos numéricos para Cálculo y diseño en Ingeniería.*, vol. 4, no. 4, pp. 497–522, 1988.

[16] D. M. Potts and L. Zdravkovic, “Some Pitfalls when using Modified Cam Clay,” in *Processdings from COST C7 Workshop*, 1999, p. 14.

[17] J. Suebsuk, S. Horpibulsuk, and M. D. Liu, “Modified Structured Cam Clay: A generalised critical state model for destructured, naturally structured and artificially structured clays,” *Computers and Geotechnics*, vol. 37, no. 7–8, pp. 956–968, Nov. 2010.

[18] M. D. Liu and J. P. Carter, “A structured Cam Clay model,” *Canadian Geotechnical Journal*, vol. 1332, no. 2002, pp. 1313–1332, 2006.

[19] S. W. Sloan, A. J. Abbo, and D. Sheng, “Refined explicit integration of elastoplastic models with automatic error control,” *Engineering Computations*, vol. 18, no. 1, pp. 121–154, 2001.

[20] Y. C. Fung, *Foundations of Solid Mechanics*, Prentice-H. New Jersey: Prentice-Hall, Inc., 1965, p. 525.

[21] M. Nazem, J. P. Carter, D. Sheng, and S. W. Sloan, “Alternative stress-integration schemes for large-deformation problems of solid mechanics,” *Finite Elements in Analysis and Design*, vol. 45, no. 12, pp. 934–943, Oct. 2009.

[22] D. M. Potts and A. Gens, “A critical assessment of methods of correcting for drift from the yield surface in elasto-plastic finite element analysis,” *International Journal for Numerical and Analytical Methods in Geomechanics*, vol. 9, pp. 149–159, 1985.